FEASIBILITY TESTS OF A VACUUM SYSTEM FOR SPring-8-II

K. Tamura[†], M. Masaki, H. Ohkuma[*], M. Shoji, Y. Taniuchi, JASRI, Hyogo 679-5198, Japan
T. Bizen, M. Oishi and S. Takahashi, JASRI/RIKEN SPring-8 Center, Hyogo 679-5148, Japan

Abstract

For SPring-8-II, the major upgrade of SPring-8 [1, 2], a test half-cell including permanent/electro magnets and a vacuum system was constructed [3], and hardware feasibility tests were performed by the end of October 2018. This paper overviews the vacuum system, mainly a stainless steel 12-meter-long integrated chamber (LIC), developed for the test half-cell, and describes vacuum performance and assembly tests conducted with the permanent/electro magnets. Investigations of inner copper plating, welding and permeability of the chambers observed by dismantling the test half-cell vacuum system are also presented.

INTRODUCTION

SPring-8, the third generation synchrotron radiation (SR) facility, has started the user operation in 1997. Since then, while making various improvements on the accelerators and beamlines, SPring-8 has been continuing stable and reliable operation. However, in order to meet the user's demand desiring higher brilliant and more coherent SR, R&D for SPring-8-II was launched and a five-bend achromat lattice design at an electron energy of 6 GeV was proposed. Estimated value of the emittance with the damping effect by insertion devices is 100 pm·rad, which enables to result in tens of higher brilliance compared with current SPring-8. Hardware was also designed to accommodate to the proposed lattice design, considering minimization of a blackout period of the user operation due to replacement of the existing storage ring with new one.

Main features of the SPring-8-II vacuum system are 1) introduction of the concept of a stainless steel (SS) 12-meter-long integrated chamber (LIC) with welded structure, and 2) adoption of ex-situ baking of the chamber [4]. We designed the 12-m LIC with a narrow aperture, flangeless structure and a minimum number of bellows so that the vacuum system could be installed without interference with the magnets of a narrow bore diameter aligned on common girders with a severe packing factor. In order to realize a short blackout period as possible, the 12 m-LIC is planned to be moved into the accelerator tunnel with maintaining ultra-high vacuum (UHV) by closing thin gate valves (Transport Gate Valve: TGV) attached at both ends, after ex-situ baking and NEG activation.

As a last stage of the hardware developments for SPring-8-II, we constructed a test half-cell to investigate the feasibility of each sub-system and check the interferences with the magnet systems. The next section outlines the test half-cell vacuum system, and the following sections describe the results of feasibility tests, dismantling investigations of the test half-cell vacuum system.

TEST HALF-CELL VACUUM SYSTEM

Figure 1 shows a layout of the test half-cell vacuum system. The 12-m LIC consists of five unit chambers, three straight section chambers (SSC2, SSC3 and SSC4) and two bending section chambers (BSC1 and BSC2) integrated by TIG welding. Two unit chambers (SSC1 and BSC3) have CF4-1/2 flanges at both ends. They are placed between an insertion device chamber and a 12-m LIC, and between two 12-m LICs, respectively.

Typical cross section of a beam chamber of SSC is 30 mm × 16 mm octagon of 2 mm thickness with a 5 mm height slot and an antechamber as shown in Fig. 2. The inner top and bottom surfaces of the beam chamber are plated with copper more than 100 μm thick to reduce the resistive wall impedance. Any SSCs consist of five parts. They are jointed in a sequence by laser beam welding (LBW) with low-heat input, which makes it possible to produce a chamber with less cross-sectional deformation and bending. Since there is only a clearance of 0.5 ~ 1 mm between the chamber and the magnet poles, the chambers need to be produced with tight mechanical tolerances to keep the clearance. Each chamber was manufactured with a straightness of 1 mm or less per 2 m in length.
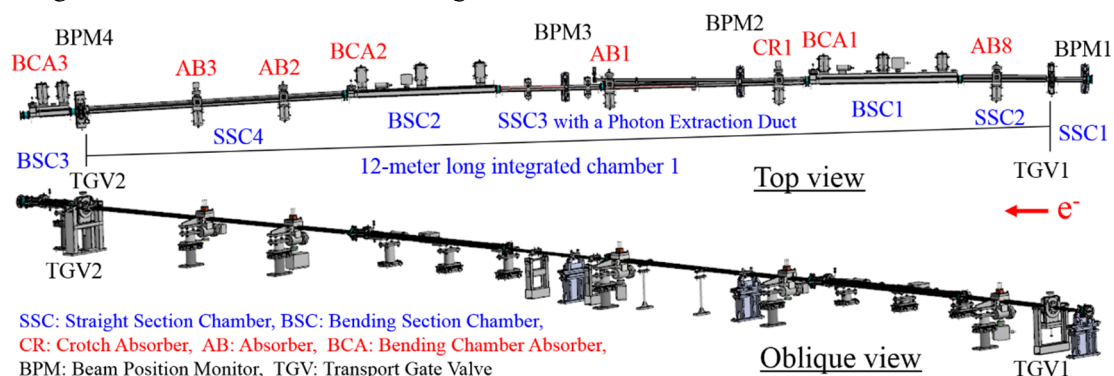
Figure 1: Test half-cell vacuum system.

---

† tamura@spring8.or.jp
* Present address: RCNP, Osaka University, Ibaraki,
Osaka 567-0047, Japan / Aichi-SR, Seto, Aichi 489-0965, Japan
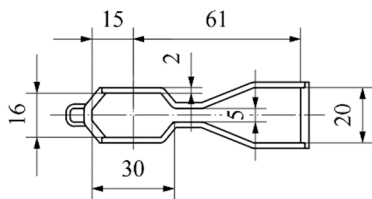
Figure 2: Cross-sectional drawing of a straight section chamber with a beam chamber of 30 mm × 16 mm for the test half-cell vacuum system.

Most of parts of each unit chamber were annealed at 900 °C for 10 minutes in the production process for lowering the relative permeability raised by processing to 1.05 or less, and also for reducing thermal gas desorption.

BPMs are not equipped in the test half-cell vacuum system. Dummy blocks without pickup electrodes were installed instead, which were prepared for verification of handling during transportation of the 12-m LIC, and also alignment and cabling after assembly of the test half-cell.

SR emitted from a bending magnet passes through the slot and antechamber, and is absorbed by discrete photon absorbers without hitting the vacuum chamber inner wall. There are three types of photon absorbers: BCA (bending section absorber), CR (crotch absorber) and AB (absorber). Each BCA is located at the end of BSCs and inserted from the outside of the BSCs to cut SR from an upstream bending magnet. CR1 and ABs are inserted into SSCs from the upside. Outgases due to photon stimulated desorption are localized around the photon absorbers and efficiently evacuated by UHV pumps discretely placed near the photon absorbers. We mainly adopted conventional Non-Evaporable Getter (NEG) cartridge pumps (Saes getters: CapaciTorr D 400-2) for main vacuum pumping. Sputter ion pumps (SIPs) for the evacuation of methane and noble gases were also installed together with the NEGs. Various types of SIP were tested to verify their pumping capabilities. For CR1 and BCA3, we choose NEXTorr D 500-5 and D 200-5, combination pumps of a NEG and a SIP produced by Saes getters, for validation of its vacuum performance. By using these UHV pumps, it was estimated that the static pressure after 150 °C baking would reach down to levels of 1e-8 Pa.

Pressures are measured by cold cathode gauges (CCGs, Pfeiffer: IKR060, IKR270, or Ampere: CCTG-110S) near every photon absorber except for BCA2. The lower limits of their measurement range are 1e-8 Pa for IKR060 and CCTG-110S, 5e-9 Pa for IKR270.

FEASIBILITY TESTS

Ex-situ Baking

Integration of five unit chambers to the 12-m LIC by TIG welding was carried out on an assembly girder in the assembling room at the SPring-8 site. A baking oven was mounted around the 12-m LIC on the assembly girder, and the 12-m LIC was ex-situ baked at 150 °C with a hot air flow. After cooling down of the 12-m LIC, all NEGs were activated and all SIPs were operated. After UHV pumps start-up, the 12-m LIC reached UHV, and all CCGs showed under the lower measurement limits.

Transportation and Assembly Test

While maintaining UHV, the 12-m LIC was hung on a strong beam, placed on a transport truck, and transported from the assembling room to the SPring-8 experimental hall where the test half-cell would be assembled. The 12-m LIC with the strong beam was lifted from the transport truck by two overhead cranes and fitted into the lower halves of the multipole magnets already aligned on three common girders (Fig. 3). After placing the 12-m LIC in the appropriate longitudinal position, two connection chambers (SSC1 and BSC3) attached to the TGVs were pumped down with two TMPs independently and baked at 150 °C in-situ. After cooling down of them to room temperature, they were connected to the 12-m LIC with UHV condition by opening the TGVs, and the vacuum conditioning of the test half-cell vacuum system was completed.

Figure 3: The 12-m LIC hung on a strong beam going to be installed inside the lower halves of multipole magnets aligned on three common girders.

After alignments of the test half-cell vacuum system with cooling water pipes, the upper halves of the multipole magnets were reassembled (Fig. 4) and the permanent bending magnets slid into their original positions from the side. Assembly of the test half-cell was successfully performed without any interferences between the magnets and vacuum system.

Figure 4: Aligned 12-m LIC and a reassembled quadrupole magnet.

In-situ Reactivation of NEGs

In order to confirm the possibility of reactivation of NEGs by the pumping with the nearest SIPs, in-situ reactivation of NEGs of the test half-cell vacuum system without TMPs was tried after venting the system with dry nitrogen and pumping down by a TMP.

All NEGs were successfully reactivated with the nearest SIPs. Ultimate pressure after reactivation of NEGs reached under the lower measurement limits of the CCGs again.

Chamber Vibration

With cooling water flowing through all multipole magnets and the whole vacuum system, the chamber vibration was measured by a velocimeter (Geospace: Geophone GS-11D). We also measured the chamber vibration of current SPring-8 employing the aluminum chamber, and confirmed that the magnitudes of both chamber vibrations were comparable. According to the method proposed by Matsui *et al.* [5], we estimated the reduction factor, which is an index of the magnitude of the influence of the chamber vibration on the beam vibration as shown in Fig. 5. It was concluded that the influence of the chamber vibration of the test half-cell vacuum system made of SS on the beam vibration is 1/10 or less of that of current SPring-8 even if the magnetic field gradient of the quadrupole magnets is taken into consideration.
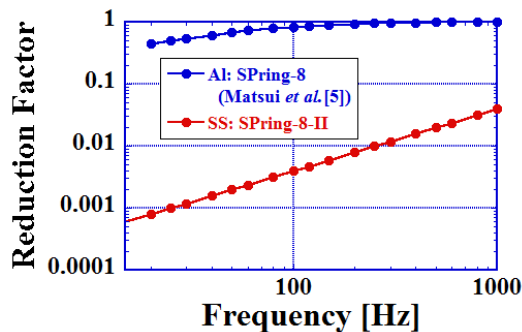
Figure 5: Comparison of reduction factor of Al chamber (SPring-8) [5] and SS chamber (test half-cell of SPring8-II).

DISMANTLING INVESTIGATIONS

After completion of all feasibility tests, the test half-cell vacuum system was finely dismantled and investigated in detail on the following four points.

Copper Plating

Thickness and adhesion were investigated for copper plating applied to the inner surface of the beam chamber for reduction of the resistive wall impedance. In a wire-cut chamber manufactured as one duct, a part of the SSC3, thickness of copper plating on the upper and lower surfaces was unbalanced and the thinner one was less than 100 μm in thickness. It is considered that adjustment of the distance between the electrode and the surfaces to be plated was insufficient. On the other hand, in the normal SSCs, since the upper and lower halves of the chambers were separately plated with copper, there was no significant difference in the thickness of the copper plating. There was no problem with the adhesion of the copper plating in either type of chamber.

LBW and TIG Welding

Microscopic observation of cross sections of laser beam welds and TIG welds was carried out for soundness investigation. In laser beam welding, the welding position deviated from the welding groove as welding progressed and a sufficient penetration depth was not secured. This is caused by insufficient teaching of the LBW system before welding, or the groove shift that occurs during welding. To solve this problem, it is essential to introduce the LBW system that automatically tracks the welding groove. In TIG welding, it was confirmed that almost proper welding was performed with either welding rod (Inconel or SS).

Steps

Steps in the welds which lead to an increase in the geometrical impedance were measured by a digital height gauge. It was confirmed that the step of each TIG weld was substantially within the specified value of 0.3 mm.

Permeability

An increase in permeability can cause disturbances in the magnetic field distribution. Since the vacuum chambers assembled with TIG welding cannot be annealed due to the existence of bellows, BPMs etc., suppression or exclusion of effects of the permeability rise due to TIG welding is essential. In case of welds using a SS welding rod, the relative permeability of some welds exceeded the specified value of 1.05, but they were the welds designed to locate outside the magnetic field. The relative permeability of the welds using an Inconel welding rod was all within the specific value.

SUMMARY

As a part of hardware developments for the construction of SPring-8-II, a test half-cell vacuum system was manufactured and its vacuum performance was verified. In addition, the vacuum system was transported while maintaining UHV, and the feasibility tests of assembling the test half-cell in combination with the permanent/electro magnets were successfully performed. The knowledge obtained from the developments is also expected to be expanded to the vacuum technology of accelerators for further advanced synchrotron radiation field.

REFERENCES

[1] H. Tanaka *et al.*, in *Proc. 7th Int. Particle Accelerator Conf. (IPAC'16)*, Busan, Korea, May 2016, pp. 2867-2870. doi:10.18429/JACoW-IPAC2016-WEPOW019

[2] K. Soutome *et al.*, in *Proc. 7th Int. Particle Accelerator Conf. (IPAC'16)*, Busan, Korea, May 2016, pp. 3440-3442. doi:10.18429/JACoW-IPAC2016-THPMR022

[3] T. Watanabe *et al.*, in *Proc. 9th Int. Particle Accelerator Conf. (IPAC'18)*, Vancouver, Canada, Apr.-May 2018, pp. 4209-4212. doi:10.18429/JACoW-IPAC2018-THPMF061

[4] M. Oishi *et al.*, in *Proc. 7th Int. Particle Accelerator Conf. (IPAC'16)*, Busan, Korea, May 2016, pp. 3651-3653. doi:10.18429/JACoW-IPAC2016-THPMY001

[5] S. Matsui *et al.*, Jpn. J. Appl. Phys. 42 (2003) pp. L338-L341.

MC7: Accelerator Technology

T14 Vacuum Technology